17th CIRP Conference on Modelling of Machining Operations

Analysis and modelling of trochoidal milling in Inconel 718

Edouard DUCROUX[a], David PRAT[a], Fabien VIPREY[a],

Guillaume FROMENTIN[a], Alain D'ACUNTO[b]

[a] Arts et Métiers ParisTech, LaBoMaP, UBFC, F-71250, Cluny, France
[b]Université de Lorraine, CNRS, Arts et Métiers ParisTech, LEM3, F-57000 Metz, France

* Corresponding author. Tel.: +33 385 595 330; fax: +33 385 595 370. *E-mail address:* edouard.ducroux@ensam.eu

Abstract

Trochoidal path increases productivity, tool life and reduces cutting forces compare to classical slot milling. Consequently, this strategy is well adapted to improve the milling performance in refractory alloy such as Inconel 718. The tool path complexity affects the tool radial engagement and axes dynamic, so it appears difficulties to perform such strategy. Therefore, this article deals with an analytical approach of trochoidal modelling to determine the theoretical radial depth of cut, cut thickness, cutting forces and machine tool behavior in function of the different methods to program the trochoidal trajectory. Finally, this methodology allows the optimization of geometrical and kinematic parameters for trochoidal milling of Inconel 718.

© 2019 The Authors. Published by Elsevier B.V.
Peer-review under responsibility of the scientific committee of The 17th CIRP Conference on Modelling of Machining Operations

Keywords: Trochoidal path ; Cutting Forces Modelling ; Slot Milling ; Inconel 718

1. Introduction

The necessity for aeronautic and aerospace industry to use more refractory material forces them to develop new machining startegies. These include development in tool geometry and grade, understanding of the cutting mechanism and improvement in machining trajectory. Research has been done to push cutting parameters such as feeds and depth of cut while producing good surface quality, improving tool life and avoiding vibrations [1].

Nomenclature

Referentials

$R_o = \{O, \underline{X}_{Machine}, \underline{Y}_{Machine}, \underline{Z}_{machine}\}$
        Workpiece referential
$R_F = \{O_T, \underline{e}_1, \underline{e}_2, \underline{e}_3\}$ Frenet referential of the trajectory
$R_{Tool} = \{O_T, \underline{X}_{tool}, \underline{Y}_{tool}, \underline{Z}_{tool}\}$ Tool referential
$R_{TRA} = \{O_S, \underline{N}_{Ps}, \underline{N}_{Pr}, \underline{I}_{Ps \cap Pr}\}$ Local discretisation referential

Trochoidal parameters

ω_{troch} Angular speed of the trajectory (rad.s^{-1})
θ_{troch} Angle described by the tool centre along the trajectory
R_{troch} Radius of the tool centre trajectory
P_{troch} Step of the tool centre trajectory

Tool parameters

Z   Number of teeth of the tool
z_{ce} Altitude of a cutting edge point in the R_{Tool} referential (mm)

Cutting parameters

a_e Tool radial engagement (mm)
h   Cut thickness (mm)

Geometrical objects

$\underline{TCT}[\theta_{troch}]$ Tool centre trajectory
$\underline{CC}_{TCT}[\theta_{troch}]$ Contact cutting point of trajectory
$\underline{CE}_{ref}[z_{ce}]$ Cutting edge reference profile

$CE[i_z, z_{ce}]$	i^{th} cutting edge profile
$R_{out}[i_z]$	i^{th} cutting edge runout
$CET[i_z, z_{ce}, \theta_{sp}]$	i^{th} cutting edge trajectory
$NL_{CET}[i_z, z_{ce}, \theta_{sp}]$	Normal vector with respect to CET

Trochoidal toolpath improves the tool life with a decreasing of the force magnitude [2]. The previous work has shown that the mechanics of trochoidal milling allows the use of the total flute length by reducing the radial depth of cut. As the cutting forces are restricted, it is possible to increase the feedrate to have a better productivity [3]. Therefore, it has been quickly used to machine slots and pockets in refractory materials such as Inconel 718 [4].

Trochoidal milling model can be separated into two different programming approaches, the circular segment trajectory model (CST) and the true trochoidal trajectory (TTT).

The CST model is the first model studied for predicting cutting forces [5]. This study focus on the computation of the radial depth of cut a_e to examine the tool load along the toolpath. It has been identified that the tool is out of cut for more than 50% of the time during the trochoidal milling. Thus, a double trochoidal path is tested where the tool goes in a direction for the first part of the arc and then in the opposite direction for the rest [6]. This toolpath increases the productivity but also the cutting forces and it affects the dynamic stability of the milling process due to the alternation in milling direction.

More recently the TTT which allows better dynamic conditions [7] has been analysed in terms of toolpath generation as it is challenging in programming and used method of interpolation to precisely represent the toolpath.

Most of the researches focuses on the prediction of the cutting forces based on the tool engagement calculation, with considering only the tool envelop. Few researches have been done to calculate the cut thickness h and tool radial engagement, i.e. the radial depth of cut a_e [8]. This allows a better forces prediction but leads to longer computation time. These researches has not analysed the CST model which is still used in some industrial process. Moreover the difference between the two trajectory models has never been investigated.

This article contains a development of trochoidal milling model for both different approaches (TTT and CST), focusing on the time determination of the radial depth of cut and the cut thickness. Then, a dynamic analysis of the machine solicitation is performed to examine which of the two trajectories is the most demanding. Finally a mechanical analysis with a force prediction model is proposed.

2. Study parameters

During the model construction and the experiments the tool used is a solid carbide end-mill from Mitsubishi Materials (IMX10C4HV100R10010S EP7020). It is a 10 mm diameter D_{Tool} end mill with 4 teeth (Z), a nose radius of 1 mm and a 45° flute angle. The tool is modeled according to the methodology detailed in [9] to define the referential cutting edge CE_{ref} as a function of z_{ce} in the tool referential R_{Tool}.

The cutting parameters, presented in Table 1, are set in order to limit the engagement angle to 20°, considering a compromise between tool life and productivity.

Table 1. Cutting parameters.

Cutting speed	Feed per tooth	Depth of cut	Trochoidal radius	Trochoidal step
V_c	f_z	a_p	R_{troch}	P_{troch}
m.min^{-1}	mm.rev^{-1}.tooth^{-1}	mm	mm	mm
60	0.1	5	1	0.05

The machined material is an Inconel 718 with a hardness of 45 HRC and a mechanical strength of 1300 MPa.

3. Trochoidal milling model

3.1. True trochoidal trajectory parametrisation

The tool center trajectory (TCT) for the true trochoidal trajectory towards the machine axis is defined by the equations (1) in R_0 referential with ω_{troch} the angular speed of the TCT and *m* the milling mode equal to 1 in down milling and -1 in up milling.

$$\begin{cases} X_{troch}[t] = \dfrac{P_{troch}}{2\pi} \omega_{troch} \cdot t + R_{troch} \cos[m \cdot \omega_{troch} \cdot t] \\ Y_{troch}[t] = R_{troch} \sin[m \cdot \omega_{troch} \cdot t] \end{cases} \quad (1)$$

A Frenet referential $\{O_T, \underline{e}_1, \underline{e}_2, \underline{e}_3\}$ is linked to the trajectory to follow the tool center O_T along it. The Fig. 1 represents the TCT generated.
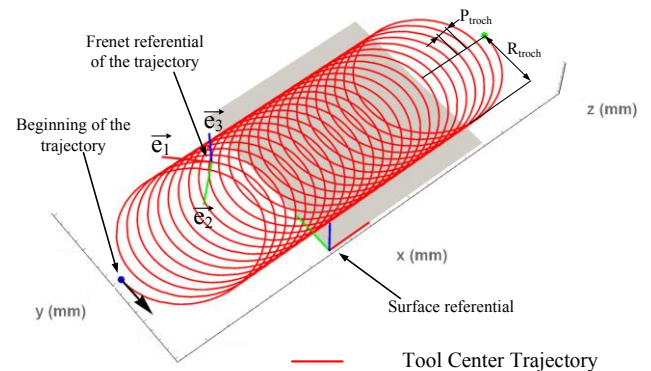

Fig. 1. True trochoidal trajectory (TTT).

With this formulation, the ω_{troch} angular speed has to be not constant in order to set the feed rate constant and equal to V_f set point. There is no analytical solution, as a consequence an approximate value of ω_{troch}, given by equation (2) is proposed with L_{troch} the length of the trochoidal curve for one revolution. The error on the real feed rate can be evaluated in function of the couple of parameters (R_{troch}, P_{troch}) as presented in Fig. 2.

$$\omega_{troch} = \frac{2\pi \cdot V_f}{60 \cdot L_{troch}} = \frac{2\pi \cdot V_f}{60 \int\limits_{0}^{T} \left\| \frac{dTCT}{dt} \right\| dt} \qquad (2)$$
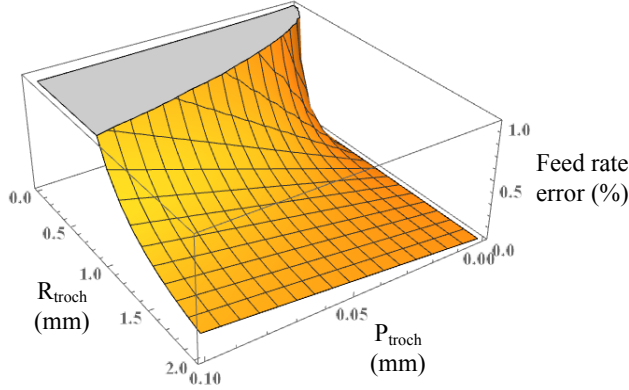

Fig. 2. Error on the modelled feed rate towards R_{troch} and P_{troch} with $V_f = 764$ mm.min^{-1}.

For the chosen set of parameters the estimated error is equal to 0.4%. This approximation would not be accurate anymore if P_{troch} becomes higher than R_{troch}. Thereafter the parametrization will be towards $\theta_{troch} = \omega_{troch}.t$ with ω_{troch} constant.

3.2. Circle-Segment trajectory parametrisation

In order to model a circular milling motion, a combination of a circular interpolation and a segment is used as shown in Fig. 3.
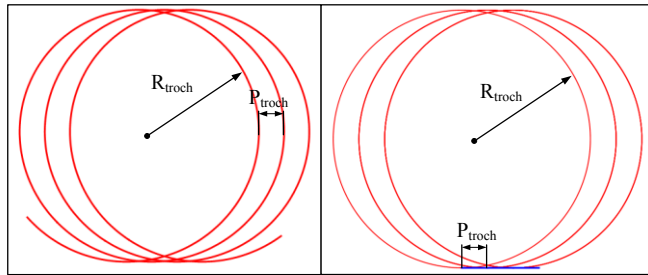

Fig. 3. Trajectories (a) TTT and (b) Circle-Segment CST.

The CST is an easier CNC programming method for trochoidal milling, nevertheless it has a curvature discontinuity between the segment and the circle.

3.3. Tool radial engagement calculation

The tool radial engagement is calculated using the trajectory of the contact cutting point which is obtained by equation (3) in R_0 referential.

$$\underline{CC_{TCT}}[\theta_{troch}] = \underline{TCT}[\theta_{troch}] - \frac{1}{2}D_{Tool}\underline{e_2}[\theta_{troch}] \qquad (3)$$

The vector $\underline{e_2}$ correspond to the normal vector to $\underline{CC_{TCT}}$. The tool radial engagement for the position $\theta_{troch,1}$ is the

distance between the effective out point of the cutting edge at this position and the one at the position $\theta_{troch,2}$ for the previous trochoid. Therefore, the position $\theta_{troch,2}$ is the solution of the intersection between the normal vector $\underline{e_2}$ at the position $\theta_{troch,1}$ and the $\underline{CC_{TCT}}$ for the previous trochoid as presented in Fig. 4. The tool radial engagement is calculated by solving equation (4) at a position near $\theta_{troch,1}$-2π.

$$\begin{cases} \underline{CC_{TCT}}[\theta_{troch,1}] = \underline{CC_{TCT}}[\theta_{troch,2}] \\ \qquad\qquad + a_e[\theta_{troch,1}] \cdot \underline{e_2}[\theta_{troch,1}] \\ \theta_{troch,2} \approx \theta_{troch,1} - 2\pi \end{cases} \qquad (4)$$
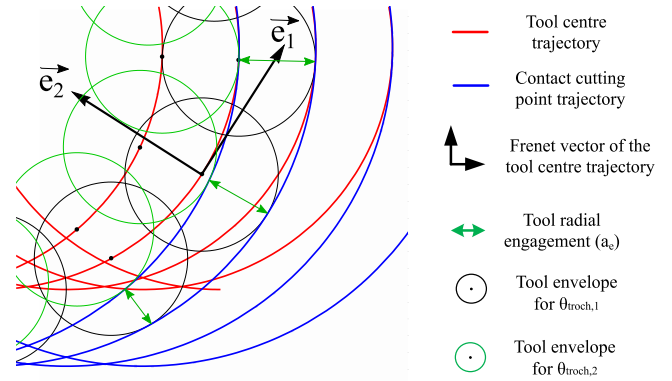

Fig. 4. Tool radial engagement construction.

Then the model need to limit the computation to the position $\theta_{troch,1}$ where the tool is indeed engaged in the workpiece. Thus all positions where the a_e computed in equation (4) is negative indicate that the direction of $\underline{e_2}$ is not anymore from $\theta_{troch,1}$ to $\theta_{troch,2}$ but the inverse. These positions correspond to the back of the trochoidal toolpath so the a_e radial engagement will be equal to 0. The tool radial engagement computed for one trochoid revolution is presented in Fig.5. It demonstrates the progressive tool engagement of trochoidal strategy.
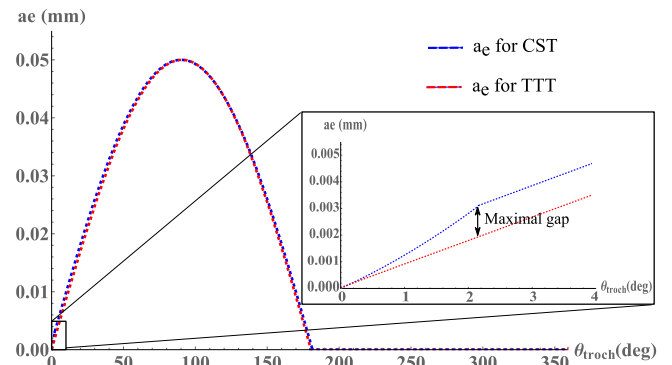

Fig. 5. Tool radial engagement (a_e) calculated for one trochoid.

Based on a_e engagement analysis, the main difference is located in the zone where the CST has the connection between the segment and the circle with a maximum of 0.0009 mm at θ_{troch} equal to 2.2°. But this difference is very slight (4.9 % mean difference) and the evolution of the

computed engagement has quite the same shape for both trajectories.

3.4. Cut thickness calculation

For the next step of the model, it needs to express all the previous variables, which depend on θ_{troch}, as a function of the spindle rotation angle θ_{sp}. Therefore, the equation (5) allows such transformation with considering no sliding between the spindle rotation and the trochoidal movement.

$$\frac{\theta_{troch}}{\omega_{troch}} = \frac{\theta_{sp}}{\omega_{sp}} \tag{5}$$

The cutting edge geometry $\underline{CE}_{ref}$ parametrized by z_{ce} height can be extended to all i_z cutting edges with radial runout $\underline{R}_{Out}$ and the variable pitch of the tool ψ considering equation (6).

$$\underline{CE}[i_z, z_{ce}] = \underline{\underline{Rot}}\left[\frac{2\pi}{Z}(i_z - 1) + \psi[i_z]\right] \cdot \underline{CE}_{ref}[z_{ce}] + \underline{R}_{Out}[i_z] \tag{6}$$

Then, from the mill rotation and the $\underline{TCT}$, the i_z^{th} cutting edge trajectory can be described by equation (7) in the R_0 referential.

$$\underline{CET}[i_z, z_{ce}, \theta_{sp}] = \underline{TCT}[\theta_{sp}] + \underline{\underline{Rot}}[\theta_{sp}] \cdot \underline{CE}[i_z, z_{ce}] \tag{7}$$

Considering the surface generated by $\underline{CET}$ of the i_z^{th} edge, the h cut thickness is the normal distance between this surface and the surface generated by the $(i_z-1)^{th}$ edge. Thus by construction of the normal line vector $\underline{NL}_{CET}$ of the surface generated by $\underline{CET}$, h is determined by finding the intersection between $\underline{NL}_{CET}$ and $\underline{CET}$ of the $(i_z-1)^{th}$ edge, which is the solution of equation (8) at a position $\theta_{sp,2}$ near $\theta_{sp,1}+(2\pi/Z)$.

$$\begin{cases} \underline{CET}[i_z, z_{ce}, \theta_{sp,1}] = \underline{CET}[i_z - 1, z_{ce}, \theta_{sp,2}] \\ \qquad + h[i_z, z_{ce}, \theta_{sp,1}] \cdot \underline{NL}_{CET}[i_z, z_{ce}, \theta_{sp,1}] \\ \theta_{sp,2} \approx \theta_{sp,1} + \dfrac{2\pi}{Z} \end{cases} \tag{8}$$

In the same manner as the tool radial engagement, the cut thickness computation is limited to the positions where the cutting edges are machining. Firstly, where $\underline{NL}_{CET}$ direction is opposite to $\underline{CET}$ of the $(i_z-1)^{th}$ edge, h cut thickness calculated is negative, the value has been replaced by 0. Secondly where a_e engagement is equal to 0, h cut thickness is equal to 0, likewise where z_{ce} height is higher than the axial depth of cut a_p. Finally, to find where the cutting edge is in materials, as presented in Fig. 6, the

model needs to compute the intersection of $\underline{CET}$ with $\underline{CC}_{TCT}$ of the previous trochoid which correspond of the entry point of the i_z^{th} edge.
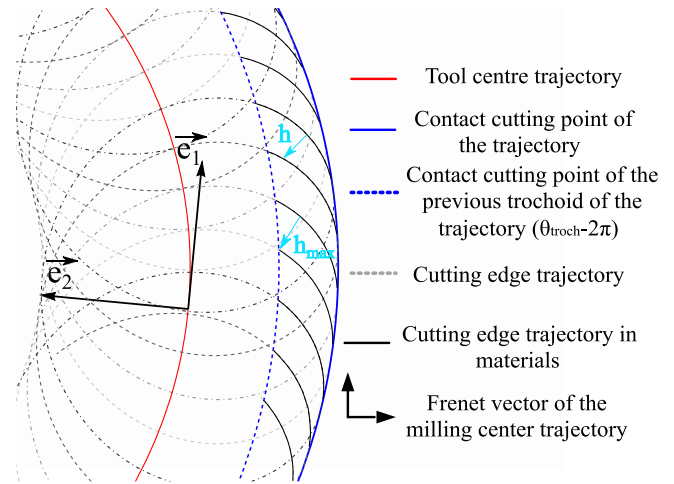

Fig. 6. Cut thickness h along edges trajectories.

The cut thickness h determined in the case of the TTT toolpath for one trochoid loop is presented in Fig. 7. As the tool radial engagement difference between CST and TTT is slight, the cutting thickness is the same for both trajectories.
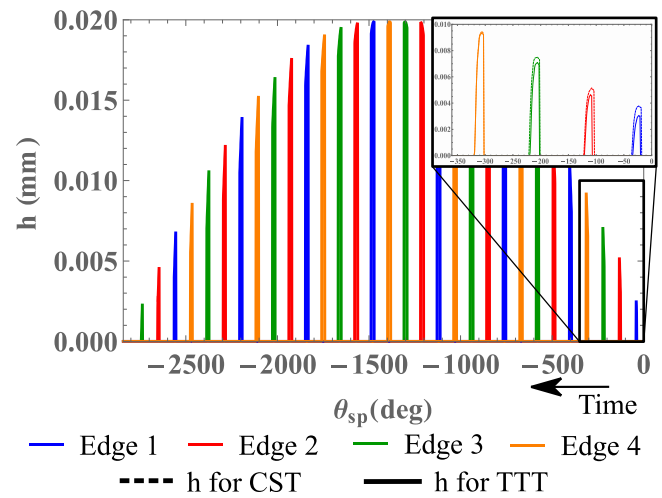

Fig. 7. Cut thickness calculated for one trochoid loop and for $z_{ce} = 1$ mm in down milling.

4. Mechanical analysis

4.1. Cutting forces model

From the calculation of the h cut thickness, a force model has been developed via the tool discretisation method to get the cutting forces in R_{TRA} presented in Fig. 8. In agreement with the norm ISO 3002-1:1993 [11], the referential $R_{TRA,j}$ linked to the jth local segment of the edge is composed by the normal at the P_r plane, the normal at the P_s plane, and the directional vector of the intersection between these two planes.
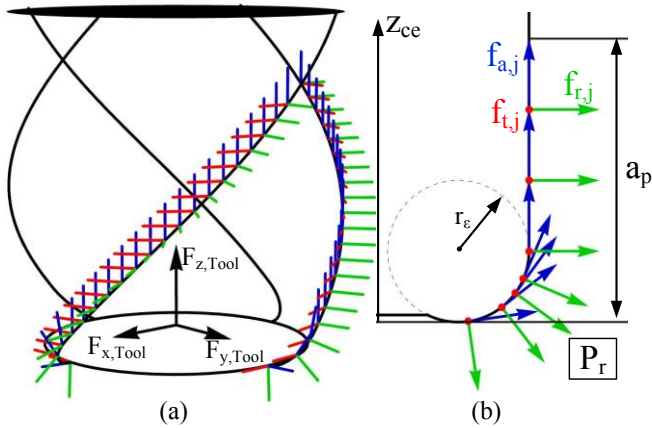
Fig. 8. Cutting edge discretisation method, illustrated in the case of cylindrical end mill.

The k component (t, r, a) of the local cutting forces in $R_{TRA,j}$ is done by equation (9).

$$\left\{f_{k,j}\left[i_z, z_{ce}, \theta_{sp}\right]\right\}_{TRA,j} = b\left(K_{kb} + K_{kh} \cdot h_j\left[i_z, z_{ce}, \theta_{sp}\right]\right)$$
(9)

Then the coefficients of the cutting law (9) have been identified through inverse identification tests according to [12] in side milling configuration. Thus the set of coefficients is presented in Table 2.

Table 2. Cutting law coefficients in R_{TRA}

Force component	f_t	f_r	f_a
K_{kb} (N.mm^{-1})	62	60	45
K_{kh} (N.mm^{-2})	2550	41	-8

4.2. Cutting forces experiment and comparison

The experiments have been performed on a Mikron HSM600U five-axis milling machine equipped by a iTNC530 Heidenhain CNC. The machine dynamic limitations are presented in Table 3.

Table 3. Machine dynamic limitations

Machine axes	Speed	Acceleration	Jerk
	(mm.min^{-1})	(m.s^{-2})	(m.s^{-3})
X axis	40 000	10	100
Y axis	40 000	10	100
Spindle	24 000 rpm		

The experiments are performed using a Kistler 9257B piezoelectric dynamometer with a sampling frequency of 50 kHz. The cutting forces have been recorded and modeled in the R_o referential. The Fig. 9 presents the measurements and the model of the cutting forces in trochoidal milling with the error
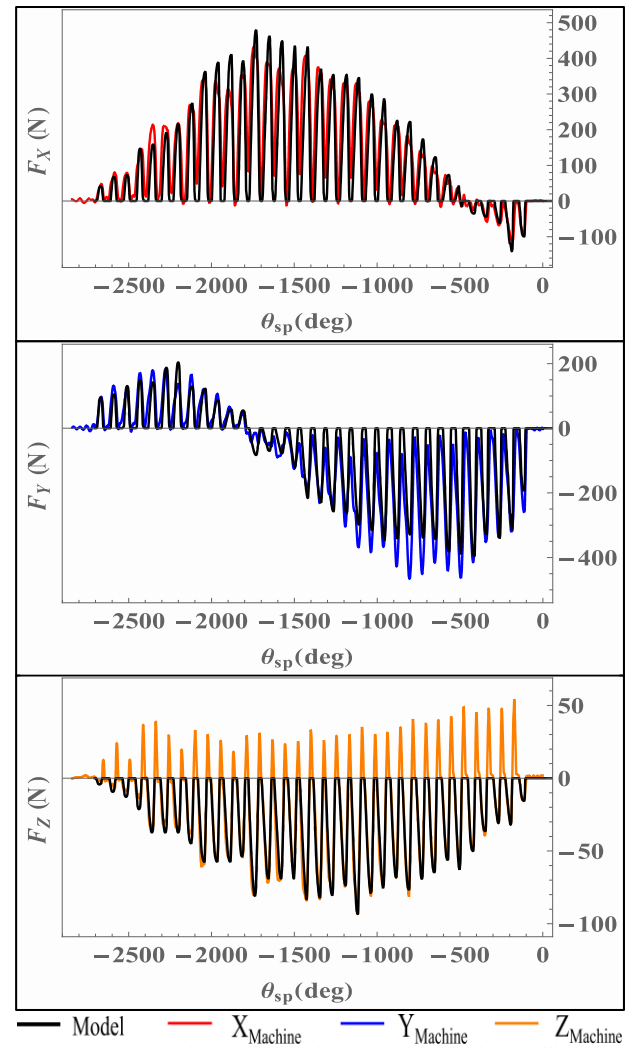

Fig. 9. Cutting forces modelled and measured in down milling
(Vc = 60 m.min^{-1}, fz = 0.1 mm.rev^{-1}.tooth^{-1}, ap = 5 mm, R$_{troch}$ = 1 mm, P$_{troch}$ = 0.05 mm).

The model shows good results in predicting cutting forces. Nevertheless the experiment presents non negligible forces in the positive direction of $Z_{Machine}$, which can be seen in [6] in other proportion. These forces can be due to multiple factors such as tool wear, chip flow or built-up edge formation.

5. Dynamic analysis

Firstly both trajectories are tested with the set of parameters presented in part 2, the machine axes dynamic are recorded by a CNC recorder software with the X-axis as the slot direction and the Y-axis as the orthogonal-slot direction. The results are presented in Fig. 10 where the model, the nominal and the effective curves respectively corresponded to the successive derivation of the position, the CNC command and the measure done.
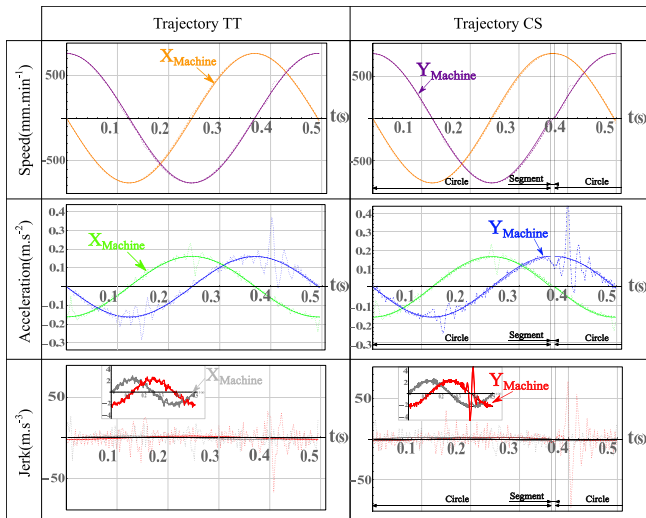
Fig. 10. Dynamic of the axis machine during trochoidal milling for $V_f = 764$ mm.min^{-1}.

It shows that the Jerk is the more likely to limit dynamically the machine as the speed and the acceleration recorded are way lower than the machine limitations. Moreover the CST seems to be more demanding than the TTT, specifically just after the curvature discontinuity, even if the machine try to compensate by decelerating and accelerating few milliseconds before and after it. Otherwise the results are close. That's why more (R_{troch}, V_f) parameters have been tested to observe the evolution of the Jerk. The parameter P_{troch} has been set to 0.05 mm to ensure a maximum engagement angle lower than 20°. The Fig. 11 presents the maximum jerk towards (R_{troch}, V_f) for the model, the measurements on the machine-tool of the CST and the TTT.
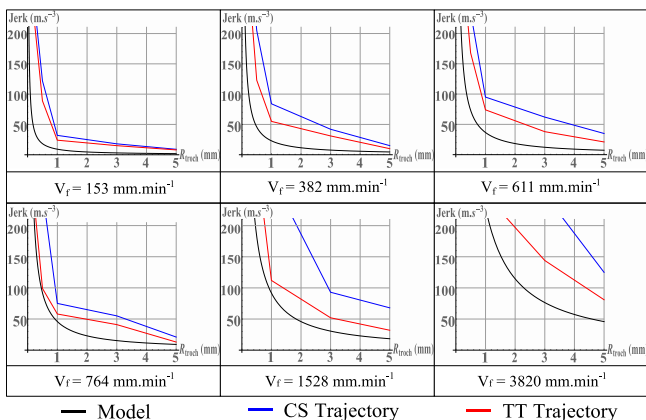

Fig. 11. Maximum jerk function of R_{troch} for different feed rates.

The analysis shows the CST induces higher axis dynamics than the TTT, then CST is more susceptible to be limited by the machine tool performances. Besides the higher the feed rate is, the more limited is the CST compared to the TTT.

6. Conclusions

The present study proposed an analytical formulation for modelling the tool radial engagement and cut thickness in trochoidal milling towards the circular approach and the true trochoidal one. This model is based on the definition of the cutting edge geometry and trajectory in order to predict cutting forces with using the discretization method.

In terms of mechanic, trochoidal milling implies a progressive variation of radial engagement helpful for reducing tool or workpiece vibrations and then is interesting for hard material milling application. The difference between the two trajectories is slight as the tool radial engagement along them is very near equal.

In terms of dynamic, the CST toolpath reach faster the machine limits and shows much more instability than the TT trajectory. This can lead to an increase of the vibration and the forces magnitude during the tool entry. Therefore a decrease of the tool life will may be observe.

Acknowledgements

References

[1] Altintas Y (2012) Manufacturing automation: metal cutting mechanics, machine tool vibrations, and CNC design. Cambridge University Press
[2] Ibaraki S, Yamaji I, Matsubara A (2010) On the removal of critical cutting regions by trochoidal grooving. Precision Engineering, 34(3):467-473
[3] Kardes N, Altintas Y (2006) Mechanics and Dynamics of the Circular Milling Process. J of Manuf Science and Engineering 129(1):21-31.
[4] Pleta A, Mears L (2016) Cutting Force Investigation of Trochoidal Milling in Nickel-based Superalloy. Procedia Manufacturing, 44th North American Manufacturing Research Conference 5:1348-1356
[5] Wu B.H, Zheng C.Y, Luo M, He X.D (2012) Investigation of trochoidal milling nickel-based superalloy. Mat Science Forum 723:332-336
[6] Otkur M, Lazoglu I (2007) Trochoidal milling. Int J Mach Tools Manuf 47(9):1324-1332
[7] Rauch M, Duc E, Hascoet J-Y (2009) Improving trochoidal tool paths generation and implementation using process constraints modelling. Int J Mach Tools Manuf 49(5):375-383
[8] Niaki A, Pleta A, Mears L (2018) Trochoidal Milling: Investigation of a New Approach on Uncut Chip Thickness Modeling and Cutting Force Simulation in an Alternative Path Planning Strategy. Int J Adv Manuf Technol 97(1):641-656
[9] Fromentin G, Poulachon G (2010) Geometrical Analysis of Thread Milling-part 1: Evaluation of Tool Angles. Int J Adv Manuf Technol 49(1):73−80
[10] Fromentin G, Poulachon G (2010) Geometrical Analysis of Thread Milling-part 2: Calculation of Uncut Chip Thickness. Int J Adv Manuf Technol 49(1):81-87
[11] ISO 3002-1 (1993) Basic quantities in cutting and grinding, Part 1: Geometry of the active part of cutting tools - General terms, reference systems, tool and working angles, chip breakers.
[12] Dorlin T, Fromentin G, Costes J-P (2016) Generalised Cutting Force Model Including Contact Radius Effect for Turning Operations on Ti6Al4V Titanium Alloy. Int J Adv Manuf Technol 86:3297–3313